



**HAL**  
open science

## Atmospheric circulation compounds anthropogenic warming and its impacts in Europe

Davide Faranda, Gabriele Messori, Aglaé Jézéquel, Mathieu Vrac, Pascal Yiou

► **To cite this version:**

Davide Faranda, Gabriele Messori, Aglaé Jézéquel, Mathieu Vrac, Pascal Yiou. Atmospheric circulation compounds anthropogenic warming and its impacts in Europe. 2021. hal-03456537v1

**HAL Id: hal-03456537**

**<https://hal.science/hal-03456537v1>**

Preprint submitted on 30 Nov 2021 (v1), last revised 21 Mar 2023 (v3)

**HAL** is a multi-disciplinary open access archive for the deposit and dissemination of scientific research documents, whether they are published or not. The documents may come from teaching and research institutions in France or abroad, or from public or private research centers.

L'archive ouverte pluridisciplinaire **HAL**, est destinée au dépôt et à la diffusion de documents scientifiques de niveau recherche, publiés ou non, émanant des établissements d'enseignement et de recherche français ou étrangers, des laboratoires publics ou privés.

# Atmospheric circulation compounds anthropogenic warming and its impacts in Europe

Davide Faranda<sup>1,2,3,\*</sup>, Gabriele Messori<sup>4,5</sup>, Aglae Jezequel<sup>3,6</sup>, Mathieu Vrac<sup>1</sup>, and Pascal Yiou<sup>1</sup>

<sup>1</sup>Laboratoire des Sciences du Climat et de l'Environnement, CEA Saclay l'Orme des Merisiers, UMR 8212 CEA-CNRS-UVSQ, Université Paris-Saclay & IPSL, 91191, Gif-sur-Yvette, France

<sup>2</sup>London Mathematical Laboratory, 8 Margravine Gardens, London, W6 8RH, UK

<sup>3</sup>LMD/IPSL, Ecole Normale Supérieure, PSL research University, 75005, Paris, France

<sup>4</sup>Department of Earth Sciences, Uppsala University, and Centre of Natural Hazards and Disaster Science (CNDS), Uppsala, 752 36, Sweden

<sup>5</sup>Department of Meteorology and Bolin Centre for Climate Research, Stockholm University, 106 91, Stockholm, Sweden

<sup>6</sup>Ecole des Ponts, Marne-la-Vallée, France

\*davide.faranda@lscce.ipsl.fr

## ABSTRACT

The thermodynamic effects of the global-mean anthropogenic warming on the climate system are well documented<sup>1</sup>. However, diagnosing dynamical changes such as those in atmospheric circulation patterns, remains challenging<sup>2</sup> – all the more when focusing on extreme events<sup>3,4</sup>. Here, we study 1948–2020 trends in the frequency of occurrence of atmospheric circulation patterns over the North Atlantic. We identify a positive feedback of the circulation that favours extreme events in Europe under anthropogenic forcing. Only a small number of atmospheric circulation patterns display significant trends in frequency of occurrence in recent decades, yet they have major impacts on surface climate. Increasingly frequent patterns drive summertime dryness and heatwaves across Europe, and enhanced wintertime storminess in the northern half of the continent. Roughly 95% of recent heatwave-related deaths and 33% of high impact windstorms in Europe were concurrent with the atmospheric circulation patterns whose frequency of occurrence has been increasing. Atmospheric patterns which are becoming rarer correspond instead to wet, cool summer conditions across Europe and cold conditions over the northern parts of the continent. The combined effect of these circulation changes is that of a strong, dynamically-driven year-round warming over most of the continent (cf.<sup>5</sup>) and increased wintertime surface winds and precipitation in Northern Europe.

## Main

Extreme weather events exact a heavy and steadily increasing socio-economic toll on Europe<sup>6</sup>, eliciting both scientific and media interest in the atmospheric circulation patterns favouring the occurrence of heatwaves<sup>7</sup>, cold spells<sup>8</sup>, heavy precipitation<sup>9</sup> and windstorms<sup>10</sup>. The question of whether, how and why these circulation patterns have been changing under anthropogenic forcing, including the role of Arctic Amplification, has been the source of a lively discussion<sup>11–15</sup>.

Of particular interest is whether atmospheric circulation patterns favouring specific extreme events have become more persistent. There are several arguments in support of an increasingly persistent summer atmospheric circulation<sup>3,16,17</sup>, which is highly relevant for the study of heatwaves<sup>18,19</sup>. The picture for the winter season is more debated<sup>11,15</sup>. A complementary line of work has analysed the frequency of occurrence of specific atmospheric circulation patterns associated with extreme events<sup>20</sup>. Heatwaves have again been a focus<sup>21,22</sup>, on account of their intimate link with the large-scale atmospheric circulation and rapidly increasing frequency and duration<sup>23</sup>. Other extremes, including as extratropical cyclones, have also been studied<sup>24,25</sup>. The two perspectives of persistence and frequency of occurrence are intimately related, since recurrence in a specific pattern translates to some extent into persistent weather and vice-versa<sup>19</sup>.

Previous efforts in the detection of atmospheric circulation shifts have often focused on the average behaviour<sup>3,11,15</sup>, or on a specific set of extreme events or circulation patterns<sup>5,18,22</sup>. Here we initially focus on the whole set of atmospheric circulation patterns in 73 years of sea-level pressure reanalysis data<sup>26</sup>, and then select those displaying significant occurrence trends (see Methods). The vast majority (92%) of circulation patterns show no significant trend in the selected/historical period; 3.6 % show increasing trends and 4.1 % show decreasing trends. Notwithstanding their rarity, the circulation patterns with significant trends have major implications for surface climate. To isolate the effect of circulation changes we consider detrended and

deseasonalized reanalysis data (see Methods) for 2 meter temperatures, daily precipitation rates, sea-level pressure and 10 meter horizontal winds over the period 1948–2020.

During both the boreal summer (June–August) and winter (December–February) seasons, the patterns with significant trends show highly coherent surface climate anomalies over Europe. Specifically, patterns occurring more frequently in winter (Fig. 1a) show a large north-south cyclonic-anticyclonic dipole. They are associated with considerably warmer wetter and windier conditions in Northern and Eastern Europe and warmer, drier conditions in Southern Europe (Fig. 1a, c, e). The yearly average temperature and precipitation associated with these patterns have no occurrence trends (Fig. 1g). Patterns occurring less frequently in winter (Fig. 1b) have a cyclonic structure in the mid-Atlantic leading to cooler (resp. warmer) temperatures over Northern (resp. Southern) Europe (Fig. 1d) and wetter (resp. drier) conditions in southern (resp. northern) Europe (Fig. 1f). The circulation patterns occurring less frequently are further associated with decreasing temperature and precipitation anomalies (Fig. 1h; significance of the trends depends on the chosen variable as discussed in the Methods).

In summer, increasingly frequent circulation patterns are associated with a large anticyclonic anomaly over continental Europe and a cyclonic anomaly offshore of the British Isles (Fig. 2a). Such circulation patterns drive warm and dry conditions over the continent (Fig. 2c,e). Circulation patterns associated with decreasing occurrence trends show a ridge of high pressure anomalies over the Atlantic and a large cyclonic structure over Northern Europe (Fig. 2b), associated with negative temperature (Fig. 2d), and positive precipitation (Fig. 2f) anomalies across most of the continent. Only weak trends appear in continental precipitation or temperature associated with any of the above patterns (Figs. 2g, h). We underline that these results are obtained for detrended datasets meaning that the observed signals are chiefly related to the atmospheric circulation.

The same analysis is repeated using the detrended 500 hPa geopotential height data (See Extended Data Figs 1 and 2) to ensure robustness of our results with respect to the choice of observable for the atmospheric circulation<sup>22</sup>. Only 13.2% of the days with positive and 18.2% of the days with negative occurrence trends are common to both sea-level pressure and 500 hPa geopotential height data. Nevertheless, there is a strong resemblance of the spatial anomaly composites for patterns with increasing or decreasing frequency of occurrence in both variables, as well as the associated impacts on temperature, winds and precipitations (cf. Figs fig:summer, fig:winter and Extended Data Figs 1 and 2). We conclude that our qualitative results are therefore robust to the choice of the observable used to diagnose the atmospheric circulation.

The surface climate anomalies associated with increasingly or decreasingly frequent circulation patterns can be directly related to the occurrence of high-impact summertime heatwaves and wintertime stormy weather in Europe. We draw high-impact heatwaves and the associated excess deaths from the EM-DAT disaster database<sup>27</sup> (see Methods). We identify 228 heatwave days over the analysis period. 10.5% of these days correspond to atmospheric circulation patterns increasing in occurrence (versus a climatological occurrence of these patterns of 3.6%), while 1.75% correspond to decreasing occurrence trends. As a term of comparison, only 4.0% of 480 cold spell days match atmospheric circulation patterns increasing in occurrence, in line with climatology. The 228 heatwave days occur during 10 major heatwave episodes, associated with 83,475 deaths. Only 1 of the selected heatwaves includes days with negative occurrence trends, while 4 of the heatwaves include an above-average fraction of days with positive occurrence trends (see Methods). The latter heatwaves are responsible for 95 % of the heatwave-related excess deaths<sup>28</sup> (Fig. 3a). Excluding the summer 2003 heatwave, which alone accounts for the bulk of the total heat-related deaths in Europe in the period considered, we still find that heatwaves associated with circulation patterns with positive occurrence trends are responsible for 55.1% of total excess deaths. Although this heuristic argument is based on a limited sample of events, it nonetheless serves to illustrate the potential societal impact that circulation patterns with increasing occurrence trends may have, and motivates a future, more systematic impact-based analysis.

We conduct a similar analysis for 90 European windstorms which resulted in a high number of casualties and/or large insured losses, extending the storm database from<sup>29</sup> (see Methods). Over a total of 438 storm days, we find that 65 (14.8%) are associated with circulation patterns with increasing occurrence trends and only 5 (1.1%) with patterns with decreasing trends. We find that 29 windstorms (33% ) show an above-average fraction of days with positive occurrence trends while 3 events (3.3%) are linked to negative trends (Fig. 3b and Extended Fig. 4) . These statistics aggregate values on a continental level. A geographically-resolved picture highlights that the proportion of storms associated with positive trends is larger in Northern Europe than in Southern Europe (Fig. 3b, e.g 40% in United Kingdom VS 0% in Italy). This is consistent with the cyclonic pattern shown in Fig. 1a).

In this paper, we identified the atmospheric circulation patterns that have become less or more likely in the historical period. We focused on the changes in the occurrence of daily patterns, rather than on conventional weather regimes or climate indices<sup>5,11,30</sup>. This allows us to detect ongoing changes in the mid-latitude atmospheric circulation, isolating significant linear trends in the frequency of occurrence of specific circulation patterns. This method is flexible, and could for example be used as a complement to extreme event attribution studies conditioned on the circulation<sup>31,32</sup>, otherwise known as the storyline approach<sup>33</sup>. The latter have been criticized for not taking into account the role of climate change-induced circulation changes<sup>34</sup>, and we provide a readily applicable toolkit to address this problem. Our approach is not data or location-specific and may be applied to different regions or datasets, in particular as a tool to evaluate the consistency of dynamical trends in numerical

91 simulations with reanalyses data.

92 An important limitation of our study is that it assumes that the circulation patterns of interest have good analogues in the  
93 dataset being used (see Methods). This assumption is problematic in the presence of strong non-stationarities which may lead  
94 to unprecedented atmospheric states. An important theoretical advance would be to complement the analysis with an analogs  
95 quality index, based on the distance between a day and its analogues.

96 We underscore that the temperatures anomalies associated with increasingly frequent circulation patterns are several times  
97 larger than the average global climate change (+1.2°C) with winter (summer) temperatures anomalies up to +7°C (+3°C) in  
98 Eastern (Western) Europe. These results are obtained when removing the seasonal cycle and a linear climate change trend, and  
99 are consistent with those obtained for the 500 hPa geopotential height in the Extended data.

100 The circulation types we study, while rare, are therefore associated with impactful extreme events, both deadly heatwaves  
101 and high-impact windstorms. While these events are not exclusively caused by circulations changes, our results show that  
102 circulation changes cannot be neglected when evaluating the consequences of climate change on extreme weather events and  
103 their impacts.

## 104 **Methods**

### 105 **Computing trends in the occurrence of atmospheric circulation patterns**

106 We use daily sea level pressure data from the NCEP/NCAR reanalysis<sup>26</sup> over the period 01/01/1948 – 31/12/2020 (26,664  
107 days). The data has a horizontal resolution of  $2.5^\circ \times 2.5^\circ$ , and we restrict our analysis to 80W – 50E and 22.5N – 70N. This  
108 corresponds to the North Atlantic and Europe, with a grid of size  $20 \times 53$ . We compute a daily climatology based on these data,  
109 and then obtain daily anomalies by subtracting the calendar daily mean from each original map. The 2 meter temperature, 500  
110 hPa geopotential height, 10 metre wind and daily precipitation rate are further detrended by removing at each grid point a linear  
111 trend on all the period considered. Significance for trends is estimated by computing the 95% confidence intervals (CI) of the  
112 fit using the Wald method<sup>35</sup>. If both the upper and lower bound of the CI for the coefficient of the fit are positive (or negative),  
113 we interpret this as a significant positive (negative) trend. None of the identified trends in Figs 1g,h) and 2g,h) is significant.  
114 Some trends in extended data Figs. 1 and 2 are significant (see legends and captions).

115 We compute the robust trends in the occurrence of atmospheric circulation patterns as follows:

- 116 1. We select a daily SLP map (note that we do not use the anomalies but the original maps).
- 117 2. We compute the Euclidean distance between daily maps, taking each daily map in turn and computing its distance from  
118 all other maps in the dataset, and define a high quantile  $q$  to select the analogues. We chose  $q = 0.98$ , meaning that we  
119 take as analogues the 2% closest fields to the target.
- 120 3. We divide the time interval of 73 years in 9 periods of roughly 8 years. We then count how many analogues  $N$  fall in  
121 each period  $t$ , obtaining  $N(t)$  with  $0 < t \leq 9$ .
- 122 4. We perform a linear fit of  $N(t)$  of the type  $at + b$ .
- 123 5. We estimate the upper and lower 95% confidence intervals CI of the  $a$  parameter of the fit. If the lower and the upper  
124 bounds of the CI for  $a$  are positive (negative), we interpret this as a significant positive (negative) trend for the selected  
125 daily SLP map and quantile  $q$ . If the confidence interval contains zero, the trend is non-significant.
- 126 6. We test the sensitivity to the choice of quantile  $q$  by repeating the above steps for  $q = 0.99, 0.995$  and retaining as daily  
127 maps with significant increasing (decreasing) occurrence trends only those having consistent (same sign AND significant)  
128 trends for all three quantiles. These are the circulation patterns that are analysed in this paper.
- 129 7. The analysis is then repeated for Z500 using the same procedures for detrending, significance and sensitivity robustness  
130 of the results.

### 131 **Computing impacts of atmospheric circulation patterns with positive occurrence trends**

132 We take heat waves and cold spells from the EM-DAT disaster database<sup>27</sup>. We focus on events over Western-Central Europe  
133 (excluding e.g. Western Russia, outlying islands such as the Canary Islands etc.), and excluded those heat waves and cold spells  
134 where no start and/or end day was provided, or which lasted only for one day. Dates included in several events were only  
135 counted once. Following these criteria, from a total of 34 heatwave episodes included in EM-DAT, we identified 228 days over  
136 10 heatwaves and 480 days over 16 cold spells.

137 European Windstorms data is taken from an updated version of the storm database of<sup>29</sup> (see Supplementary Data),  
138 which originally covered the period between 1948 and 2015. Our database is largely based on the catalogues by<sup>36</sup> and<sup>37</sup>.

139 Additional storms have been integrated from the Wikipedia web-page [https://en.wikipedia.org/wiki/List\\_of\\_European\\_windstorms](https://en.wikipedia.org/wiki/List_of_European_windstorms) because of their relevance in terms of human losses, damages or their profile in the media.  
140 Using publicly contributed databases as sources for scientific information is becoming a common practice in citizen science  
141 projects, which are gaining momentum in the geosciences<sup>38,39</sup>. Specifically, the events we have retrieved from Wikipedia are  
142 extensively referenced and documented in both scientific and news articles and reports from national meteorological services  
143 and research institutions. A detailed description of the windstorm database is provided in the Extended Data.  
144

145 To determine whether a given event is associated to analogues with positive or negative occurrence trends (i.e. an increasingly  
146 or decreasingly frequent circulation pattern), we first compute the fraction of days with positive occurrence trends within each  
147 heatwave or storm. We then compare these fractions to the average frequency of occurrence of circulation patterns with positive  
148 or negative occurrence trends within the 20 years centred on the heatwave or storm. This is because the frequency of occurrence  
149 of atmospheric circulation patterns with positive occurrence trends is by definition higher in the later part of the data than  
150 in the earlier years, such that each heatwave/storm should be compared to the period within which it occurs. Based on this  
151 comparison, we then separate events into groups which have an above or below-average fraction of daily analogues with either  
152 trend.

## 153 References

- 154 1. IPCC. *Summary for Policymakers*, book section SPM, 1–42 (Cambridge University Press, Cambridge, United Kingdom  
155 and New York, NY, USA, 2021).
- 156 2. Collins, M. *et al.* Challenges and opportunities for improved understanding of regional climate dynamics. *Nat. Clim.*  
157 *Chang.* **8**, 101–108 (2018).
- 158 3. Coumou, D., Di Capua, G., Vavrus, S., Wang, L. & Wang, S. The influence of arctic amplification on mid-latitude summer  
159 circulation. *Nat. Commun.* **9**, 1–12 (2018).
- 160 4. Dai, A. & Song, M. Little influence of arctic amplification on mid-latitude climate. *Nat. Clim. Chang.* **10**, 231–237 (2020).
- 161 5. Corti, S., Molteni, F. & Palmer, T. Signature of recent climate change in frequencies of natural atmospheric circulation  
162 regimes. *Nature* **398**, 799–802 (1999).
- 163 6. Forzieri, G. *et al.* Escalating impacts of climate extremes on critical infrastructures in europe. *Glob. environmental change*  
164 **48**, 97–107 (2018).
- 165 7. Sousa, P. M. *et al.* Distinct influences of large-scale circulation and regional feedbacks in two exceptional 2019 european  
166 heatwaves. *Commun. Earth & Environ.* **1**, 1–13 (2020).
- 167 8. Lehmann, J. & Coumou, D. The influence of mid-latitude storm tracks on hot, cold, dry and wet extremes. *Sci. reports* **5**,  
168 1–9 (2015).
- 169 9. Zanardo, S., Nicotina, L., Hilberts, A. G. & Jewson, S. P. Modulation of economic losses from european floods by the  
170 north atlantic oscillation. *Geophys. Res. Lett.* **46**, 2563–2572 (2019).
- 171 10. Hanley, J. & Caballero, R. The role of large-scale atmospheric flow and rossby wave breaking in the evolution of extreme  
172 windstorms over europe. *Geophys. Res. Lett.* **39** (2012).
- 173 11. Cattiaux, J., Peings, Y., Saint-Martin, D., Trou-Kechout, N. & Vavrus, S. J. Sinuosity of midlatitude atmospheric flow in a  
174 warming world. *Geophys. Res. Lett.* **43**, 8259–8268 (2016).
- 175 12. Horton, R. M., Mankin, J. S., Lesk, C., Coffel, E. & Raymond, C. A review of recent advances in research on extreme heat  
176 events. *Curr. Clim. Chang. Reports* **2**, 242–259 (2016).
- 177 13. Mann, M. E. *et al.* Projected changes in persistent extreme summer weather events: The role of quasi-resonant amplification.  
178 *Sci. advances* **4**, eaat3272 (2018).
- 179 14. Cohen, J. *et al.* Divergent consensus on arctic amplification influence on midlatitude severe winter weather. *Nat. Clim.*  
180 *Chang.* **10**, 20–29 (2020).
- 181 15. Riboldi, J., Lott, F., d’Andrea, F. & Rivière, G. On the linkage between rossby wave phase speed, atmospheric blocking,  
182 and arctic amplification. *Geophys. Res. Lett.* **47**, e2020GL087796 (2020).
- 183 16. Coumou, D., Lehmann, J. & Beckmann, J. The weakening summer circulation in the northern hemisphere mid-latitudes.  
184 *Science* **348**, 324–327 (2015).
- 185 17. Routson, C. C. *et al.* Mid-latitude net precipitation decreased with arctic warming during the holocene. *Nature* **568**, 83–87  
186 (2019).

- 187 **18.** Kornhuber, K. *et al.* Extreme weather events in early summer 2018 connected by a recurrent hemispheric wave-7 pattern.  
188 *Environ. Res. Lett.* **14**, 054002 (2019).
- 189 **19.** Röthlisberger, M., Frossard, L., Bosart, L. F., Keyser, D. & Martius, O. Recurrent synoptic-scale rossby wave patterns and  
190 their effect on the persistence of cold and hot spells. *J. Clim.* **32**, 3207–3226 (2019).
- 191 **20.** Horton, D. E. *et al.* Contribution of changes in atmospheric circulation patterns to extreme temperature trends. *Nature* **522**,  
192 465–469 (2015).
- 193 **21.** Jézéquel, A., Yiou, P., Radanovics, S. & Vautard, R. Analysis of the exceptionally warm december 2015 in france using  
194 flow analogues. *Bull. Am. Meteorol. Soc.* (2017).
- 195 **22.** Jézéquel, A. *et al.* Trends of atmospheric circulation during singular hot days in europe. *Environ. Res. Lett.* **13**, 054007  
196 (2018).
- 197 **23.** Perkins-Kirkpatrick, S. & Lewis, S. Increasing trends in regional heatwaves. *Nat. communications* **11**, 1–8 (2020).
- 198 **24.** Dacre, H. F. & Pinto, J. G. Serial clustering of extratropical cyclones: a review of where, when and why it occurs. *npj*  
199 *Clim. Atmospheric Sci.* **3**, 1–10 (2020).
- 200 **25.** Laurila, T. K., Gregow, H., Cornér, J. & Sinclair, V. A. Characteristics of extratropical cyclones and precursors to  
201 windstorms in northern europe. *Weather. Clim. Dyn. Discuss.* 1–34 (2021).
- 202 **26.** Kalnay, E. *et al.* The ncep/ncar 40-year reanalysis project. *Bull. Am. meteorological Soc.* **77**, 437–472 (1996).
- 203 **27.** Guha-Sapir, D. Em-dat: The emergency events database–université catholique de louvain (ucl)–cred, brussels, belgium  
204 (2017).
- 205 **28.** Fouillet, A. *et al.* Excess mortality related to the august 2003 heat wave in france. *Int. archives occupational environmental*  
206 *health* **80**, 16–24 (2006).
- 207 **29.** Faranda, D., Messori, G. & Yiou, P. Dynamical proxies of north atlantic predictability and extremes. *Sci. reports* **7**, 1–10  
208 (2017).
- 209 **30.** Cassou, C. & Cattiaux, J. Disruption of the european climate seasonal clock in a warming world. *Nat. Clim. Chang.* **6**,  
210 589–594 (2016).
- 211 **31.** Meredith, E. P., Semenov, V. A., Maraun, D., Park, W. & Chernokulsky, A. V. Crucial role of black sea warming in  
212 amplifying the 2012 krymsk precipitation extreme. *Nat. Geosci.* **8**, 615–619 (2015).
- 213 **32.** Trenberth, K. E., Fasullo, J. T. & Shepherd, T. G. Attribution of climate extreme events. *Nat. Clim. Chang.* **5**, 725–730  
214 (2015).
- 215 **33.** Shepherd, T. G. A common framework for approaches to extreme event attribution. *Curr. Clim. Chang. Reports* **2**, 28–38  
216 (2016).
- 217 **34.** Otto, F. E. *et al.* The attribution question. *Nat. Clim. Chang.* **6**, 813–816 (2016).
- 218 **35.** Stein, C. & Wald, A. Sequential confidence intervals for the mean of a normal distribution with known variance. *The*  
219 *Annals Math. Stat.* 427–433 (1947).
- 220 **36.** Lamb, H. H. & HH, L. British isles weather types and a register of the daily sequence of circulation patterns 1861-1971.  
221 (1972).
- 222 **37.** Roberts, J. *et al.* The xws open access catalogue of extreme european windstorms from 1979 to 2012. *Nat. Hazards Earth*  
223 *Syst. Sci.* **14**, 2487–2501 (2014).
- 224 **38.** Fritz, S. *et al.* Geo-wiki: An online platform for improving global land cover. *Environ. Model. & Softw.* **31**, 110–123  
225 (2012).
- 226 **39.** Sparrow, S. *et al.* Openifs@ home version 1: a citizen science project for ensemble weather and climate forecasting.  
227 *Geosci. Model. Dev.* **14**, 3473–3486 (2021).

## 228 **Acknowledgement**

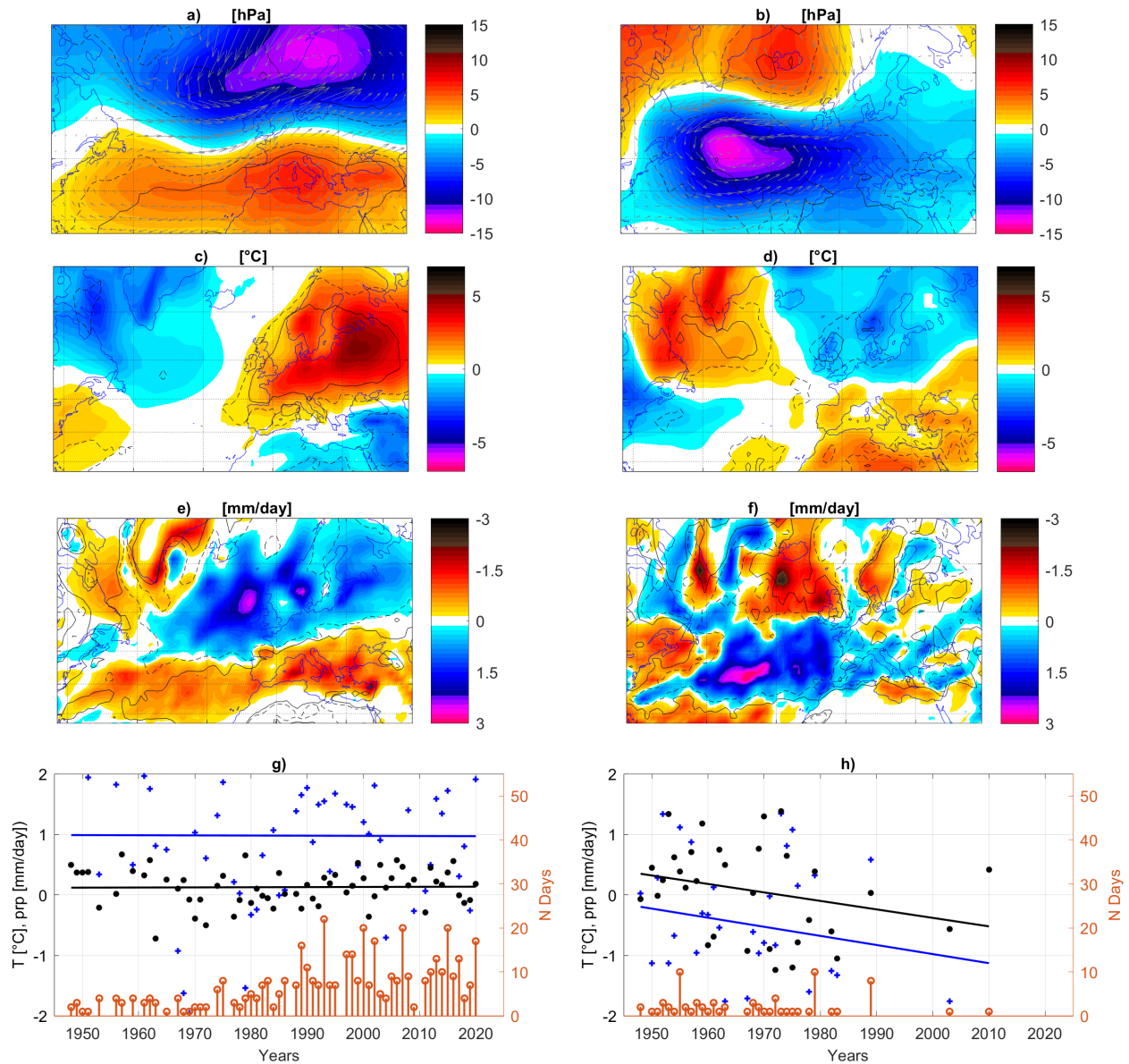
229 D.Faranda, M. Vrac, P. Yiou received funding under the European Union’s Horizon 2020 research and innovation programme  
230 (Grant agreement No. 101003469, XAIDA). D. Faranda, G. Messori and P. Yiou received funding under the European Union’s  
231 Horizon 2020 research and innovation programme, Marie Skłodowska-Curie (Grant agreement No. 956396, EDIPI). G.  
232 Messori received funding from the European Research Council (ERC) under the European Union’s Horizon 2020 research and  
233 innovation programme (Grant agreement No. 948309, CENAE). D. Faranda acknowledges the support of the ANR-TERC  
234 grant BOREAS and the LEFE-MANU-INSU-CNRS grant DINCLIC.

235 **Author contributions**

236 D.F. conceived the study, performed the bulk of the analysis and compiled the European windstorm database. G.M performed  
237 the analysis on the EM-DAT database and contributed to compiling the European windstorm database. D.F and G.M, wrote the  
238 manuscript. D.F., G.M., A.J., M.V. ad P.Y. reviewed and integrated the manuscript.

239 **Competing Interests**

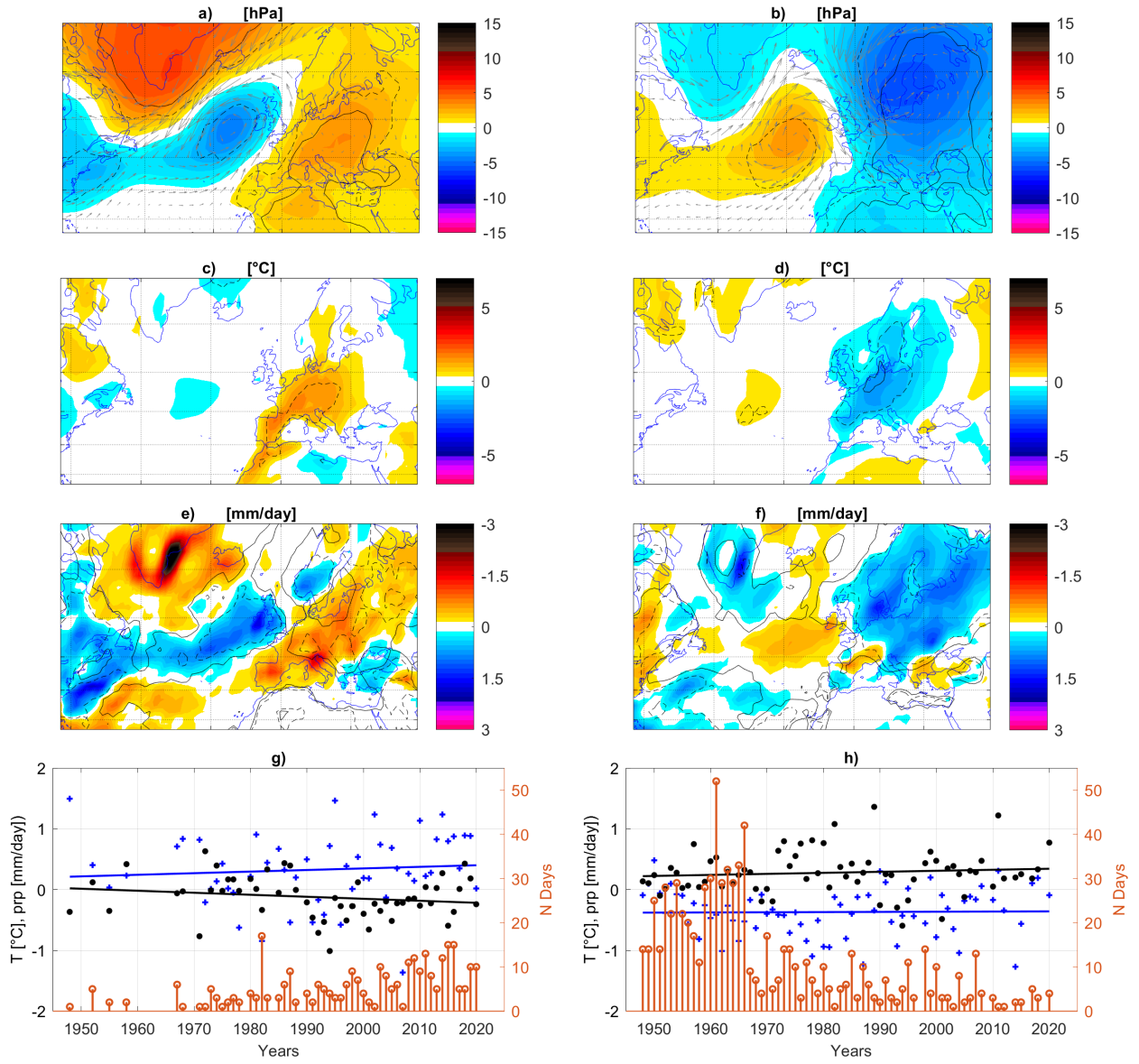
240 The authors report no conflict of interest.



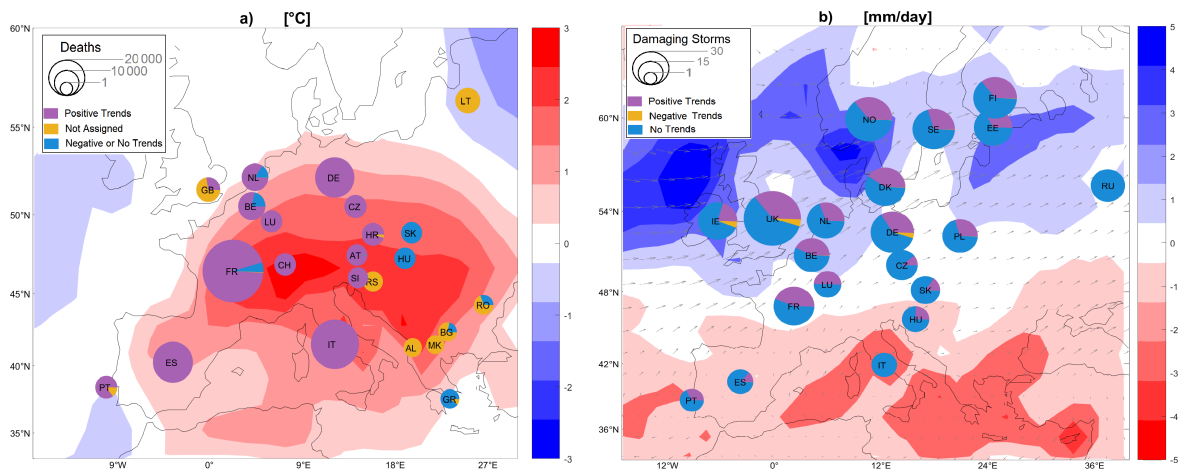
**Figure 1. Sea-level pressure wintertime atmospheric circulation patterns with significant trends in frequency of occurrence and associated surface anomalies:** Composite anomalies of DJF sea-level pressure and 10m horizontal wind (a,b), 2-meters temperatures (c,d), precipitation rates (e,f) for days with increasing (a,c,e) or decreasing (b,d,f) occurrence trends. Spatial average of yearly temperature anomalies (blue crosses) and precipitation rates (black dots) during the days with increasing (g) or decreasing (h) frequency of occurrence and count of days displaying an occurrence trend (red stems). The composites in (g), (h) are computed on all European land points (domain shows in Extended Data Fig. 3). None of the trends in (g,h) is significant. In the composite, dotted (continuous) black contours indicate regions where 2/3 (3/4) of the anomalies have the same sign. Solid lines in panels (g,h) represent linear trends.

fig:winter





**Figure 2. Sea-level pressure summertime atmospheric circulation patterns with significant trends in frequency of occurrence and associated surface anomalies:** As in Fig. 1, but for JJA. None of the trends in (g,h) is significant. 11g: summer



**Figure 3. Impacts of changing atmospheric circulation patterns during Summer in terms of heatwave casualties and European Windstorms.** (a) The size of the pie chart for each country shows the total number of heatwave excess deaths as recorded in the EM-DAT database. The purple slices show the fraction of excess deaths associated with heatwaves showing an above-average frequency of circulation patterns with a positive occurrence trend. The yellow slices show the excess deaths associated with heatwaves that we excluded from our analysis, because start or end days were missing or because only a single heatwave day was recorded in the database (see Methods). Finally, the blue slices show the corresponding fractions for heatwaves showing circulation patterns with no or negative occurrence trends. The shading on the geographical map shows the temperature anomalies ( $^{\circ}\text{C}$ ) during the 228 heatwave days retained for analysis. (b) The size of the pie chart for each country shows the total number of destructive windstorms in the storm database (see Methods). The purple slices show the fraction of storms showing an above-average frequency of circulation patterns with a positive occurrence trend. The yellow slices show the corresponding fraction for storms showing analogues with negative occurrence trends and the blue slices with no trends. The shading on the geographical map shows the precipitation anomalies ( $\text{mm day}^{-1}$ ) during the 438 windstorm days retained for analysis; vectors show  $10\text{m}$  wind anomalies ( $\text{m s}^{-1}$ ).

fig:impact

# Extended Data for: Atmospheric circulation compounds anthropogenic warming and its impacts in Europe

Daive Faranda<sup>1,2,3,\*</sup>, Gabriele Messori<sup>4,5</sup>, Aglae Jezequel<sup>3,6</sup>, Mathieu Vrac<sup>1</sup>, and Pascal Yiou<sup>1</sup>

<sup>1</sup>Laboratoire des Sciences du Climat et de l'Environnement, CEA Saclay l'Orme des Merisiers, UMR 8212 CEA-CNRS-UVSQ, Université Paris-Saclay & IPSL, 91191, Gif-sur-Yvette, France

<sup>2</sup>London Mathematical Laboratory, 8 Margravine Gardens, London, W6 8RH, UK

<sup>3</sup>LMD/IPSL, Ecole Normale Supérieure, PSL research University, 75005, Paris, France

<sup>4</sup>Department of Earth Sciences, Uppsala University, and Centre of Natural Hazards and Disaster Science (CNDS), Uppsala, 752 36, Sweden

<sup>5</sup>Department of Meteorology and Bolin Centre for Climate Research, Stockholm University, 106 91, Stockholm, Sweden

<sup>6</sup>Ecole des Ponts, Marne-la-Vallée, France

\*dave.faranda@lscce.ipsl.fr

## ABSTRACT

The extended data contain: i) additional text and references, ii) 2 additional figures

## Supplementary European Windstorm Database

European Windstorms data is taken from an updated version of the storm database of<sup>1</sup> (see Supplementary Data), which originally covered the period between 1948 and 2015. This database is largely based on the catalogues by<sup>2</sup> and<sup>3</sup>. Additional storms have been integrated from the Wikipedia web-page [https://en.wikipedia.org/wiki/List\\_of\\_European\\_windstorms](https://en.wikipedia.org/wiki/List_of_European_windstorms) because of their relevance in terms of human losses, damages or their profile in the media. We have only selected storms that have been analyzed by a meteorological office or research institute: a link to the documentation is provided. Using publicly contributed databases as sources for scientific information is becoming a common practice in citizen science projects, which are gaining momentum in the geosciences<sup>4,5</sup>. Our database includes a total of 438 storm dates and 90 distinct storms or storm clusters. Extended Figure 4 presents the database per country (a) and per time of occurrence (b).

The database is organized in four columns:

1. The day of occurrence in the format `yyyymmdd`;
2. The name(s) of the storm;
3. The countries or the region affected;
4. A reference to a peer-reviewed article, a report or a press article describing the importance of the storm.

As a caveat to our methodology, we note that the increasing coverage of both meteorological instruments and technological means of information results in an increasing number of storms with time.

## References

1. Faranda, D., Messori, G. & Yiou, P. Dynamical proxies of north atlantic predictability and extremes. *Sci. reports* **7**, 1–10 (2017).
2. Lamb, H. H. & HH, L. British isles weather types and a register of the daily sequence of circulation patterns 1861-1971. (1972).

3. Roberts, J. *et al.* The xws open access catalogue of extreme european windstorms from 1979 to 2012. *Nat. Hazards Earth Syst. Sci.* **14**, 2487–2501 (2014).
4. Fritz, S. *et al.* Geo-wiki: An online platform for improving global land cover. *Environ. Model. & Softw.* **31**, 110–123 (2012).
5. Sparrow, S. *et al.* Openifs@ home version 1: a citizen science project for ensemble weather and climate forecasting. *Geosci. Model. Dev.* **14**, 3473–3486 (2021).

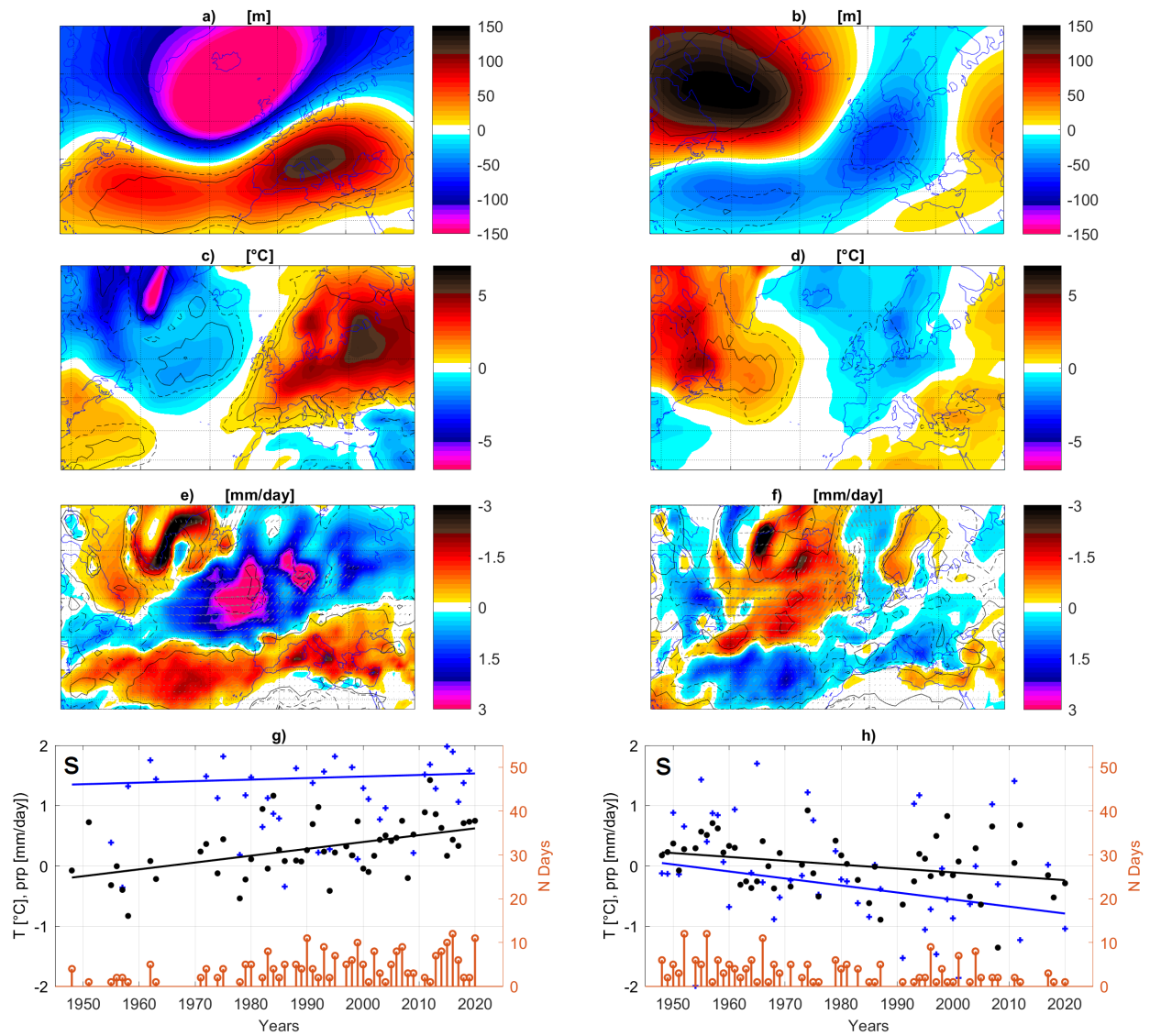


**Figure 1. 500 hPa Geopotential height wintertime atmospheric circulation patterns with significant trends in frequency of occurrence and associated surface anomalies:** As in Fig. 1, but for 500 hPa geopotential height (m). A letter 'S' of the same color of the trend lines in (g, h) indicates significance (see Methods).

fig:Z500winter

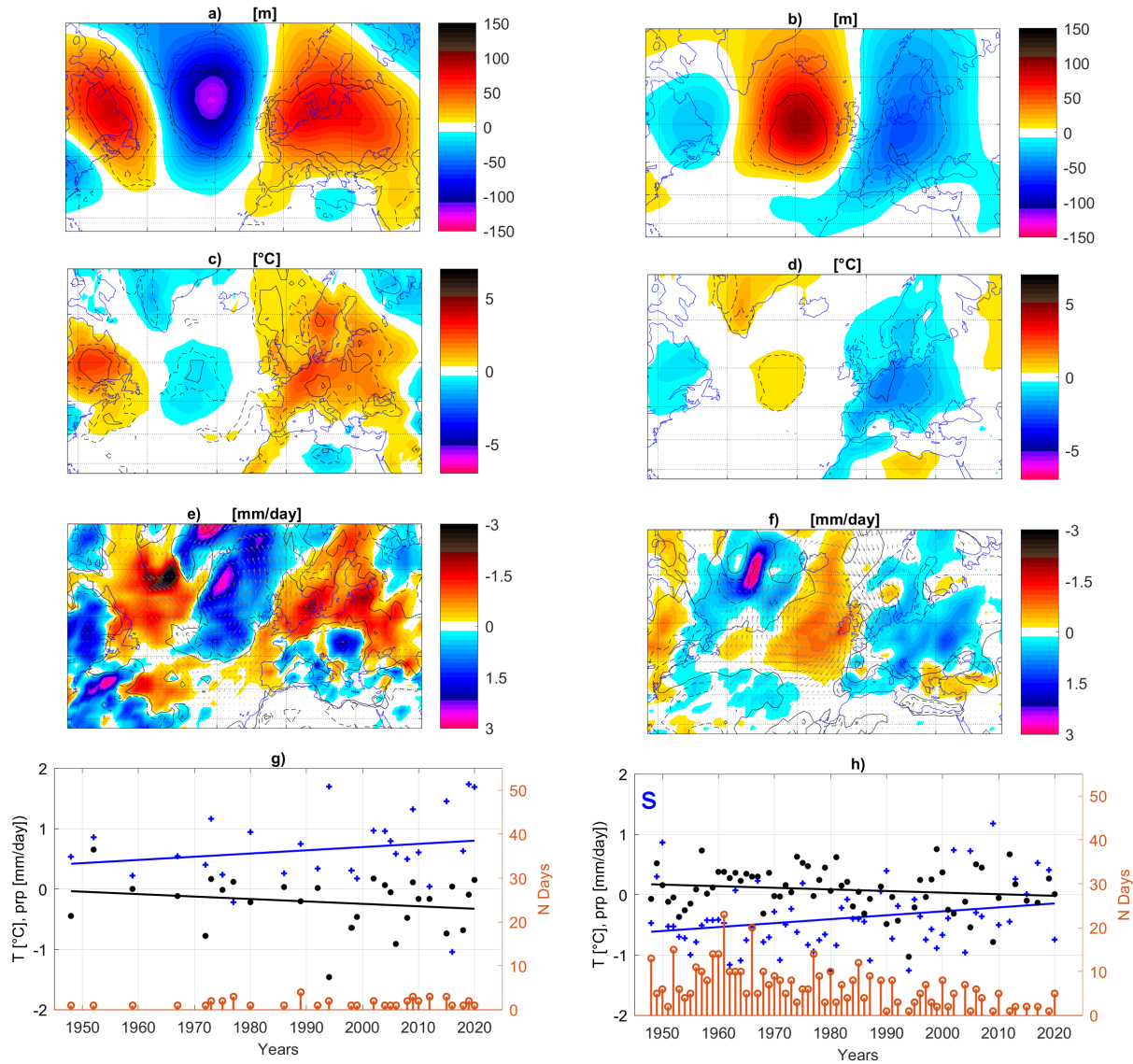


**Figure 2. 500 hPa Geopotential height summertime atmospheric circulation patterns with significant trends in frequency of occurrence and associated surface anomalies:** As in Fig. 2, but for 500 hPa geopotential height (m). A letter 'S' of the same color of the trend lines in (g, h) indicates significance (see Methods). fig:z500summer

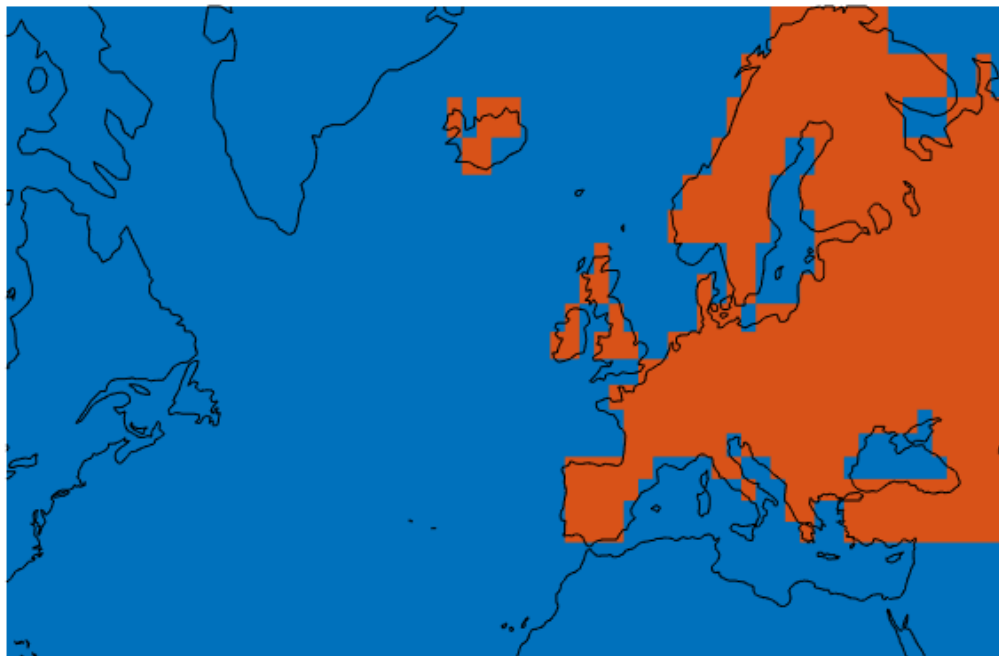


**Figure 3. European mask used to compute timeseries of continental European data:** Red shading shows the gridboxes used to compute timeseries of continental European data shown in Figs. 1,2 and Extended Figs. 1,2 panels g,h. `fig:Mask`

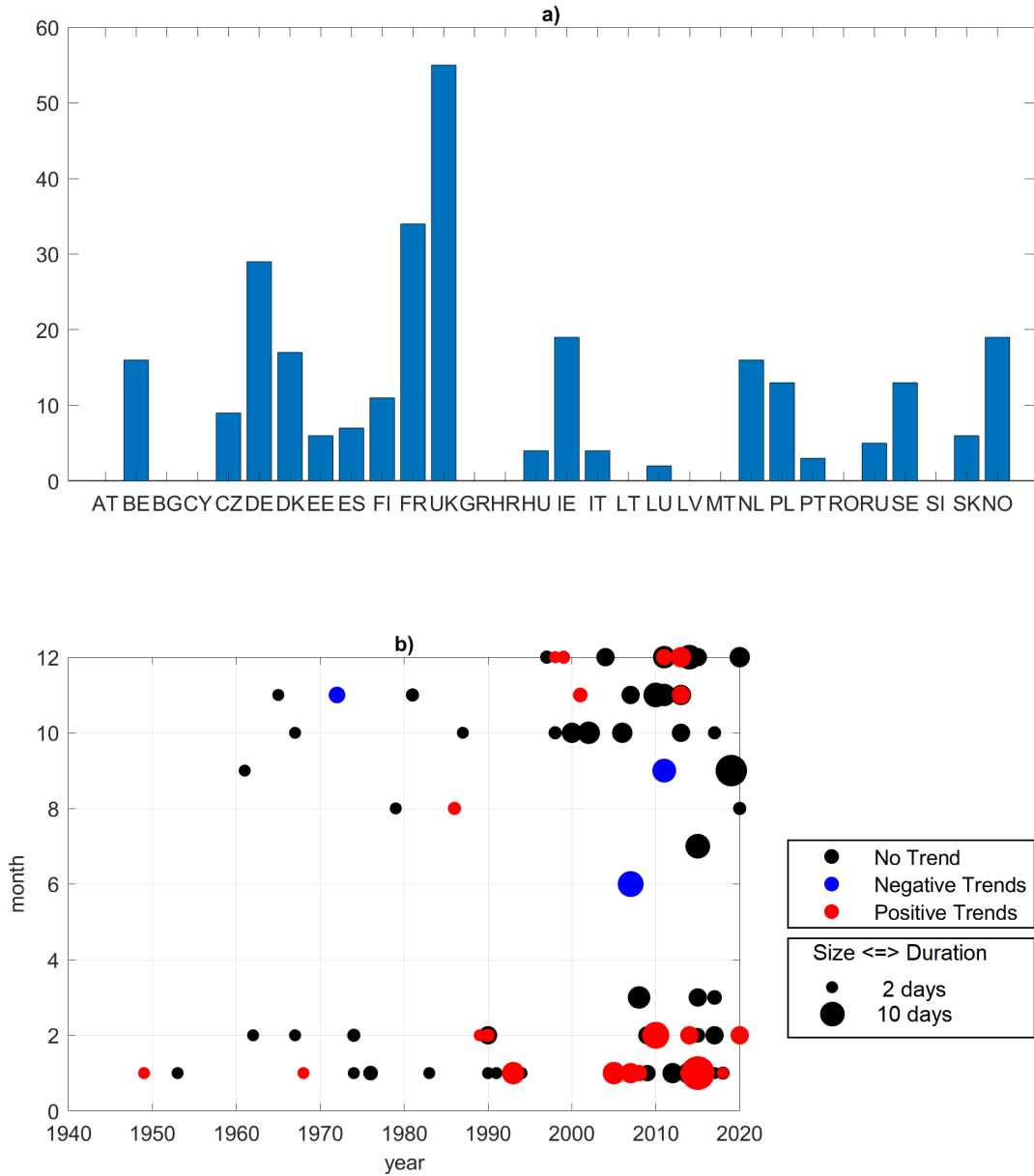


**Figure 4. Spatial and temporal distribution of European windstorms:** Number of European Windstorms per country (a). Year, month of occurrence of each storm and duration (size of the balls) and whether the storms are associated with atmospheric patterns displaying no, negative or positive trends in frequency of occurrence (colours). fig:EUstorm